

Comparison of Intraparticle Sorption and Desorption Rates for a Halogenated Alkene in a Sandy Aquifer Material

Thomas C. Harmon*

Department of Civil and Environmental Engineering, University of California—Los Angeles, Los Angeles, California 90024

Paul V. Roberts

Department of Civil Engineering, Stanford University, Stanford, California 94305

The objectives of this research were 2-fold: (1) to test the hypothesis that the rate of desorption of a halogenated alkene from a water-saturated aquifer material equals the rate of sorption in that system and (2) to develop a technique for measuring desorption rates that would be useful in characterizing a large-scale, heterogeneous subsurface environment. A batch desorption methodology (intermittent purging) was developed as an extension of a documented, long-term equilibration technique (flame-sealed ampules). A batch model incorporating radial pore diffusion with internal retardation captured the dynamics of the observed desorption behavior. However, the model consistently underestimated desorption rates at early times and overestimated rates at later times. The best-fitting effective pore diffusion coefficient values (D_p) for the Borden sand fractions ranged over nearly 2 orders of magnitude (7×10^{-10} to 5×10^{-8} cm²/s) and were, in most cases, two to four times lower than previous sorption rate estimates for the Borden sand. Possible reasons for the discrepancy are presented and discussed.

Introduction

Nonequilibrium or rate-limited desorption refers to contaminant release processes that are slow relative to the rate of groundwater flow. The necessity for incorporating such processes in a contaminant transport model is dependent on the scale of contaminated domain and the desired resolution of the model simulation. Several field studies conducted under forced gradient conditions have demonstrated the need for an understanding of rate-limited desorption processes (1-3). There is also evidence to suggest that desorption rates may control the net rate of contaminant biodegradation in an *in situ* aquifer remediation effort (4-6).

Much of the research in the area of nonequilibrium transport phenomena can be linked to early evidence of nonequilibrium sorption behavior that was inferred from the extended tailing of breakthrough curves derived from soil column experiments. In the context of these types of experiments, the concept of mobile and immobile zone transport was introduced by van Genuchten, Wierenga, and co-workers (7, 8). Their one-dimensional transport model incorporated the effects of advection, dispersion, and a source-sink term comprising the following: (1) an equilibrium expression to model the partitioning between the solid and liquid phases; (2) a first-order rate expression to model the exchange between the mobile aqueous zone and a well-mixed immobile aqueous zone. Several mathematically equivalent interpretations of the first-order rate constant have been offered (see ref 9), with the most

common one describing it as an approximation of diffusion. As evidence for an intraparticle diffusive interpretation was acquired (see the following section), a more rigorous description of the immobile zone transport, that of retarded radial diffusion, was introduced in column models (10).

Many researchers have successfully employed physical nonequilibrium models in fitting soil column data (7, 11-20). However, only a few have succeeded in modeling column breakthrough curves using independently estimated rate parameters, whether from batch experiments (15, 20, 21) or from theoretical considerations (17).

Numerous batch sorption and desorption studies have paralleled the column studies in an effort to elucidate the mechanism underlying nonequilibrium behavior. Karickhoff (22) used a continuous purging technique to study the release of several organic compounds from river sediments. Karickhoff suggested that a diffusive transfer from sorption sites inaccessible to the bulk water was responsible for the initially fast and then slow release of the compounds. Later, Karickhoff and Morris (23) studied the sorption and desorption of pyrene, pentachlorobenzene, and hexachlorobenzene to and from eight sediments. They modeled the uptake and release data using a two-site model (one fraction of rapidly equilibrating sorption sites; another fraction of slowly equilibrating sorption sites) as an approximation of a diffusive mechanism.

This study constitutes an investigation of the desorption rate of PCE from the well-studied Borden sand in an effort to: (1) demonstrate the reversibility of the sorption of nonpolar organics to aquifer materials characterized by low organic carbon content and (2) demonstrate a viable means of determining desorption rate parameters for use in aquifer remediation models.

The first goal addresses an issue recurrent throughout the literature involving observations of desorption rates varying with equilibration times and differing from observed sorption rates. Rao and Davidson (24) reviewed much of the early sorption/desorption literature and concluded that, aside from the more easily rectifiable artifacts (e.g., unsolicited chemical or biological transformations; centrifugation effects), resistant fractions (i.e., sorbed solute that is slowly desorbed, but will desorb eventually) were one of the leading causes of the observed nonsingularity of sorption/desorption behavior. Pignatello (25) also noted several prevalent artifacts, including that caused by solute sorption to colloidal solids in the aqueous portion of the sample (26, 27). Perhaps the most prevalent cause of the observed nonsingularity of sorptive uptake and desorptive release is the failure to achieve equilibrium during the sorptive uptake phase of the experiment (24, 25, 28-30).

Several desorption studies avoided the problem regarding the attainment of equilibrium by employing field-

* E-mail address: tch@seas.ucla.edu.

contaminated soils that had been subjected to years or decades of contaminant contact (e.g., refs 31–33). These researchers have also reported slow releases of contaminant and have invoked diffusion through an immobile phase as a likely cause. Lack of knowledge of the total mass associated with the field-contaminated samples limits the scope of the data interpretation in these types of studies.

The secondary focus of this work was to develop an expedient method suitable for desorption rate measurements for the relatively large number of samples that might be associated with hazardous waste site characterization. Results from several theoretical investigations have suggested that the spatial variability of equilibrium sorption parameters (i.e., distribution coefficients or retardation factors) can significantly enhance the solute spreading (34–36). The impact of the spatial variability of sorption/desorption rate parameters has not been investigated extensively, but has been shown to enhance solute spreading in computational exercises (35, 37).

Many investigators have successfully employed purging techniques to measure the rate of desorption of volatile chemicals from soil–water systems (e.g., refs 19, 22, and 38–40). The method developed in this paper employs an intermittent purging process to measure desorptive rate behavior in batch systems of saturated aquifer solids. The intermittent purging method was applied to samples composed of Borden sand and tetrachloroethene (PCE), providing a basis for comparison with a previous study of the sorption rate behavior (41).

Several studies have compared sorption/desorption equilibrium and rate parameters derived from batch and miscible flow experiments (15, 40, 42). Results indicate that if adequate time is allotted for equilibrium to be established, the two methods tend to yield the same parameter values. Young and Ball (20) recently demonstrated that, due to short column lengths and/or high flow rates, many column experiments were fairly insensitive to nonequilibrium sorption processes and could produce rate parameter estimates that did not agree with parameters derived from batch experiments. Their results suggest that while particle scale sorption and desorption mechanisms can be examined using soil column configurations, such experiments are more difficult to perform and appear to provide no more information than batch techniques. A recently developed approach (43, 44) employs a system which purges an unsaturated column and directs the effluent gas into a gas chromatograph for contaminant quantification. This system provides batch-type desorption rate data with excellent resolution, but which may be subject to the limitations discussed by Young and Ball.

Theory

In the parlance of contaminant transport, the sorption capacity of a soil or aquifer solids is given by its equilibrium partitioning coefficient or distribution coefficient (K_d , commonly reported in units of mL/g). This parameter can be estimated, with substantial uncertainty, by multiplying the organic carbon partitioning coefficient value (K_{oc}) from an empirical correlation (e.g., refs 45–48) by the organic carbon content of the soil. However, the K_d is preferably a measured value, obtained by equilibrating the soil–water suspension with a range of aqueous concentrations. For the Borden sand–PCE system, the relationship between the equilibrium aqueous and sorbed

concentrations, referred to as a sorption isotherm, is linear or nearly so over a limited concentration range (49), and the K_d value is given by the slope. The expression for a linear isotherm is given by

$$q_e = K_d C_e \quad (1)$$

where q_e is the equilibrium sorbed concentration (M_x/M_s), C_e is the equilibrium aqueous concentration (M_x/L^3), M_x is the mass of organic contaminant x , and M_s is the mass of sorbent (aquifer solid).

In some cases, a nonlinear isotherm may be more appropriate. Several isotherm models (e.g., Freundlich, Langmuir), which are based on gas adsorption theory (see ref 50), have been used empirically to describe the sorption of hydrophobic organic solutes to natural sorbents. The Freundlich isotherm is a power law that can be stated as

$$q_e = K_F C_e^{1/n} \quad (2)$$

where K_F is the Freundlich capacity coefficient [$(M_x/M_s)/(M_x/L^3)^{1/n}$] and $1/n$ is the Freundlich exponent (–). For the sorption of nonpolar organics to natural sorbents, the Freundlich exponent value is usually less than 1, indicating favorable sorption (i.e., the ratio of sorbed concentration to aqueous concentration increases as aqueous concentration decreases).

Mass Transfer Resistance. The mechanism or mechanisms controlling the slow fraction of solute uptake or release have not been conclusively verified. However, a dual-resistance model (film and intraparticle diffusion: surface and pore), in various forms, has been invoked previously to describe the hypothesized mechanism (15, 39, 41).

Generally, the dual-resistance model is insensitive to the film diffusion component in well-mixed, batch systems (15), and in most cases associated with groundwater transport (17). The relative contributions of surface and pore diffusion are more difficult to distinguish as the processes occur in parallel within the particle. Surface diffusion is commonly invoked to explain intraparticle transport that appears to be faster than could be accounted for by aqueous diffusion. Miller and Pedit (30) attempted to explain the apparent discrepancy between sorption and desorption using a reactive surface diffusion model (the solute, lindane, degraded abiotically during the course of experiments). While their model was successful in simulating the observed data, Miller and Pedit suggest that a reactive pore diffusion interpretation may be a more appropriate model for such systems. Finally, mass transport in aquifer solids usually occurs much more slowly than aqueous diffusion, so surface diffusion is usually neglected (e.g., refs 39 and 41). The following discussion assumes that pore diffusion governs the rate of release of solute from a particle.

For a sorbing solute, under transient conditions, a mass balance over a volume element of a homogeneous particle yields Fick's second law in spherical geometry:

$$\rho_a \frac{\partial q_r}{\partial t} + \epsilon_i \frac{\partial C_r}{\partial t} = \frac{\epsilon_i D_p}{r^2} \frac{\partial}{\partial r} \left(r^2 \frac{\partial C_r}{\partial r} \right) \quad (3)$$

where ρ_a is the apparent density of the sorbing particle [M_s/L^3]; q_r is the immobile sorbed-phase concentration [M_x/M_s]; ϵ_i is the fractional intraparticle porosity (–); C_r is the immobile aqueous-phase concentration [M_x/L^3]; D_p

is the effective pore diffusion coefficient [L^2/T]; and r is the radial coordinate [L]. Equation 3 can be simplified by differentiating the expression for the equilibrium isotherm (eq 1) and substituting for q_r . This substitution is valid if the rate of partitioning at the pore wall is fast relative to the rate of diffusion through the pore water (i.e., if the local equilibrium assumption is valid in the pores). The new mass balance is in terms of the aqueous concentration:

$$\frac{\partial C_r}{\partial t} = \frac{D_p}{R_{int}} \frac{1}{r^2} \frac{\partial}{\partial r} \left(r^2 \frac{\partial C_r}{\partial r} \right) \quad (4)$$

where R_{int} is the internal or grain retardation factor [-], defined by

$$R_{int} = 1 + \frac{\rho_a K_d}{\epsilon_i} \quad (5)$$

for linear equilibrium partitioning. If the Freundlich isotherm expression (eq 2) is differentiated instead of the linear expression, then the grain retardation factor is dependent on the aqueous concentration:

$$R_{int} = 1 + \frac{(1/n)\rho_a K_d C^{1/n-1}}{\epsilon_i} \quad (6)$$

In both cases, the ratio of variables in the equation for grain retardation factor is equal to the ratio of sorbed mass to aqueous mass within the immobile particle zone. The effect of a relatively larger value of a grain retardation factor is an apparently slower diffusion process (see eq 9).

The effective pore diffusion coefficient, D_p , can be further defined as

$$D_p = \frac{D_b}{\chi_e} \quad (7)$$

where χ_e is the effective tortuosity factor [-] and D_b is the bulk aqueous diffusivity [L^2/T]. D_b values are known for many organic solutes or can be accurately estimated using empirically derived correlations (e.g., ref 51). Thus, with an independent estimate of the grain retardation factor, the effective tortuosity factor (χ_e) becomes the ultimate fitting parameter for a batch system modeled using eq 4. The effective tortuosity is meant to account for the tortuous nature of pore networks and dead-end pores and for effects such as steric hindrance, in the case of extremely narrow pores.

Wakao and Smith (52) introduced a simplistic model that related the effective tortuosity to a single, measurable parameter. According to their model, the effective tortuosity factor is related inversely to the internal porosity of the sorbent (ϵ_i)

$$\chi_e = \frac{1}{\epsilon_i} = \frac{D_b}{D_p} \quad (8)$$

This relationship has failed to adequately account for the slow rates of sorption and desorption in recent studies with the Borden sand (41) and other natural sorbents (3). For some natural particles, the effective tortuosity factor may be spatially variable, as has been suggested elsewhere (53). More complex expressions than that in eq 8 have been presented in the past, mainly for porous catalysts

(e.g., refs 54 and 55). Such expressions are more specific than is warranted, as none of these pore characteristics can be independently estimated using available methods.

In the absence of independent estimates of grain retardation factors, the following expression can be substituted for eq 4:

$$\frac{\partial C_r}{\partial t} = D_a \frac{\partial}{\partial r} \left(r^2 \frac{\partial C_r}{\partial r} \right) \quad (9)$$

where $D_a = D_p/R_{int}$ is the apparent diffusion coefficient [L^2/T]. The apparent diffusion coefficient can be used to describe an overall desorption rate.

If the effective pore diffusion coefficient is independent of solute concentration, then the apparent diffusion coefficient for the linear isotherm case is a constant value, while that for the nonlinear isotherm case varies with concentration. Furthermore, it can be demonstrated via the solution of eq 9 (with eq 6) that for a given solute/sorbent system, uptake will proceed at an overall faster rate than release (56) if the equilibrium is favorable ($1/n < 1$). The observed D_a value for an uptake (sorption rate) experiment would thus be greater than the observed D_a value for a release (desorption rate) experiment.

The external boundary condition for eq 4 (or eq 9) is of particular interest, as it will affect the overall desorption rate greatly. A constant zero boundary condition maintains the maximum concentration gradient at all times and produces the fastest overall desorption rate for a given system. An external boundary comprising a well-mixed solution of limited volume will produce an initial desorption rate which is comparable to that for the early stages of the constant zero boundary conditions. However, as the bulk fluid-phase solute concentration approaches C_r ($r < a$), the concentration gradient, and thus the overall desorption rate, is greatly reduced relative to that in the constant zero boundary case. The nature of the intermittent purging method in this work (see Mathematical Modeling section) required an external boundary condition which alternates between the zero concentration and the well-mixed solution of limited volume conditions. Analytical solutions for the spherical diffusion model with either external boundary condition and with a zero-gradient internal boundary condition (concentration profile symmetry) are available (57).

Experimental Methods

The aquifer solids chosen for this study were from the Borden field site (Borden, Ontario), which has been described in detail elsewhere (58, 59). The Borden sand has been studied extensively with respect to an array of physical characteristics (60) and equilibrium sorption capacity (49, 61, 62). In a study closely related to this work, Ball and Roberts (41) measured the rate of sorptive uptake of two solutes, perchloroethene (PCE) and 1,2,4,5-tetrachlorobenzene, by bulk and fractionated Borden sand. The results from their uptake experiments serve as the point of departure for this study.

Solute and Sorbent. Tetrachloroethene, or perchloroethene (PCE), was the solute chosen for the study. PCE is a fairly recalcitrant compound and, given reasonable precautions, is suitable for use in long-term studies. PCE is resistant to aerobic degradation (63), but will degrade under methanogenic conditions (64, 65). PCE appeared

Table 1. Physical Characteristics of Borden Aquifer Material (Assembled from Ref 60)

U.S. standard mesh size	size range (mm)	nominal radius ^a (mm)	organic carbon 100f _{oc} (-)	specific SA (m ² /g)	intraparticle porosity 100 ε _i ^b (-)
-12+20	1.7-0.85	0.6	0.099	1.9	4.80
-20+40	0.85-0.42	0.3	0.052	0.88	1.91
-40+60	0.42-0.25	0.16	0.023	0.4	1.81
-60+80	0.25-0.18	0.11	0.014	0.36	1.20
-80+120	0.18-0.125	0.075	0.013	0.51	1.36
-120+200	0.125-0.075	0.048	0.015	0.36	1.52
-200	<0.075	0.03 ^c	0.035	0.9	0.35
bulk		0.011 ^d	0.021	0.42	1.31

^a Geometric mean of the mesh sizes. ^b ε_i = (Hg porosimetry porosity)/(Hg porosimetry porosity + 1/ρ_s), assuming ρ_s = 2.71 g/cm³ and ρ_a = ρ_s(1 - ε_i). ^c Geometric mean of upper limit (0.075 mm) and a lower limit of 0.045 mm (a single dry-sieving on this size mesh retained 99.6% of this fraction). ^d Sauter mean radius (76) based on size fraction contribution to bulk K_d value (41).

to resist abiotic transformation in contact with Borden sand in laboratory (49, 61) and field experiments (58).

The Borden sand for this study was taken from a set of core samples obtained from a location that was a few meters from those used in the previous sorption studies (49). The sand was dry sieved (60) into the eight size fractions shown in Table 1; the particle size distribution was the same as that for the bulk sample used previously. Ball and co-workers also characterized the sand fractions with respect to organic carbon content, specific surface area, and intragranular porosity. Their results are also employed in this work and are summarized in Table 1. Briefly, the Borden sand is characterized by an extremely small fraction of organic carbon (bulk f_{oc} = 0.0002). The values of specific surface area estimated for the Borden sand (bulk value = 0.4 m²/g) and the hysteresis observed in nitrogen gas adsorption/desorption isotherms suggested the presence of internal porosity. Mercury intrusion was used to quantify the small but measurable intragranular porosity values presented in Table 1.

Analytical Methods. The radiolabeled chemical ([¹⁴C]-PCE; Sigma Chemicals, 4.1 mmol/mCi, 99% purity) was promptly diluted in methanol and stored at -5 °C prior to use. The purity of the radiochemical was verified using gas chromatography (Packard 437A with ⁶³Ni electron capture detector, Packard Instrument Co., Downers Grove, IL; for details, see ref 56). The impurities found (1-2% of the [¹⁴C]PCE mass) were not identified and failed to volatilize under the stripping conditions detailed in the description of the intermittent purging method. The impure fraction appeared to remain in the aqueous phase (i.e., did not sorb) in a limited study of its behavior.

The aqueous PCE solutions used in spiking the samples were prepared by diluting the [¹⁴C]PCE/methanol solution in carbon-filtered, deionized water (Milli-Q system, Millipore Corp., Bedford, MA) in a gas-tight 20-mL syringe equipped with a Teflon-lined plunger. Addition of a known volume of a saturated solution of nonlabeled, reagent-grade PCE to the syringe elevated the spiking solution to the desired PCE concentration. The specific activity of the spiking solution allowed for a workable spiking volume (4-7 μL) for addition to the sample prior to the ampule sealing. All samples were counted at least two times for 20 min each (Tricarb 4350, Packard Instrument Co.).

Desorption Studies. The desorption method comprised four steps: (1) spiking and sealing the samples, (2) measuring sorptive uptake, (3) purging the aqueous phase intermittently, and (4) recovering the final mass fraction.

Ball and Roberts (41, 49) introduced the flame-sealed ampule method for determining sorptive equilibrium and

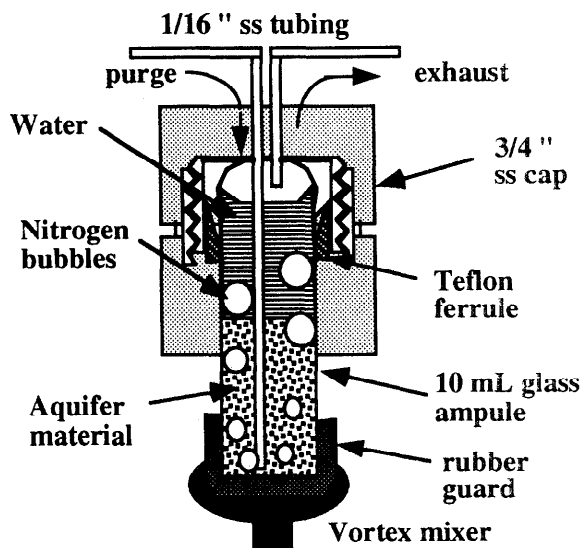


Figure 1. Schematic representation of ampule orientation on the intermittent purging apparatus: a 3/4-in. stainless steel cap fitted with influent and effluent 1/16-in. stainless steel tubes; cap equipped with Teflon ferrules.

nonequilibrium parameters with volatile organic chemicals. The method served as the precursor to the desorption rate measurements and entailed adding an approximately 1.5:1 solid to liquid ratio of Borden sand and synthetic groundwater (66) to 10-mL glass ampules. Samples were autoclaved prior to the addition of the synthetic groundwater, which was added through a sterilized 0.2-μm filter. Samples were spiked, and then the ampules were flame-sealed and incubated for time periods which at least doubled the previously determined 95% equilibration times (*t*_{0.95}, see Table 2). The mixing regime for the incubating samples resembled that developed by Bail and Roberts (41) to avoid mass transfer limitations while minimizing particle abrasion.

Prior to the ampule cracking, samples were centrifuged for 30 min at 2000 rpm. Immediately after the cracking, 1-2 mL of the supernatant was transferred into scintillation fluid, providing a measurement of the aqueous-phase concentration of the solute. This concentration then provided the basis for an estimate of the equilibrium distribution coefficient (*K*_d) and the initial conditions for the intermittent purging sequence.

Each purging apparatus or purger consisted of a 1.9-cm (3/4-in.) stainless steel cap fitted with 1.59-mm (1/16-in.) o.d., stainless steel tubing purge and exhaust conduits. A cross-sectional view of one purger is provided in Figure 1. A flow rate of 20-30 mL N₂/min was sufficient to strip the

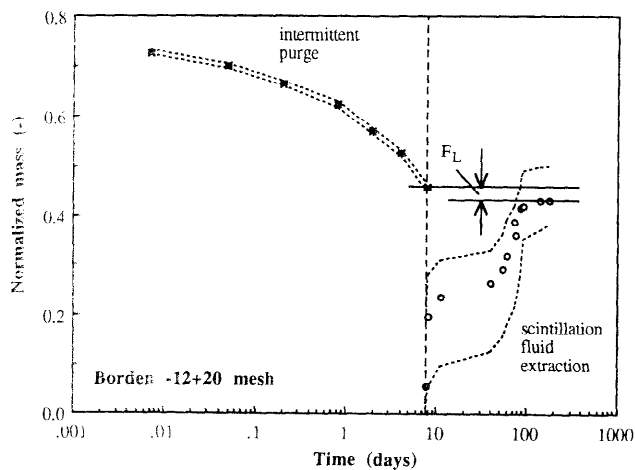


Figure 2. Estimation of the fractional loss (F_L) of PCE from a Borden -12+20 mesh sample as the difference between the fraction remaining after purging and the fraction recovered from scintillation fluid extraction (dashed lines indicate ± 1 SD at each datum).

PCE from the aqueous-phase samples in 10 min. The scintillation fluid trap (approximately 15 mL) consistently recovered approximately 99% of the PCE in this time. Samples were mixed several times (two or three for the larger size fractions; four or five for the smaller fractions) on a vortex mixer both during and between purge times to avoid the formation of concentration gradients in the interparticle pore space. More frequent mixing did not significantly increase the observed desorption rates and appeared to abrade material from the particles' surfaces.

Scintillation Fluid Extraction. Following the final purge, samples were allowed to settle, and a portion of each supernatant was delivered directly into scintillation fluid. The ampule was then shattered, and two gravimetrically determined portions of the aquifer solid sample were delivered directly into vials containing scintillation fluid. Another two portions of the solids were dried overnight at 60 °C and reweighed for an estimate of water content (generally 15–20% by weight).

The sample was recounted several times, until achievement of a maximum level of radioactivity signaled the end of the extraction phase of the experiment. In several cases, samples were monitored beyond this point to test for losses from the scintillation fluid vials. Most of the samples conserved mass over the extended periods, even when subjected to abrupt temperature changes. However, some samples did appear to lose small amounts of mass over long periods, presumably due to improper sealing of the scintillation vials. Scintillation fluid extraction data, such as that shown in Figure 2, provided a second estimate of the desorption rates. However, results using this method (not shown in this work) were less reproducible and may have been affected by the scintillation fluid achieving cosolvent levels of activity within the intraparticle pores. A more detailed account of the scintillation fluid extraction method and results is provided elsewhere (67).

Mathematical Modeling

The solution to eq 4 was approximated using an implicit finite difference scheme (Crank–Nicholson) employing a predictor–corrector routine to address the nonlinear isotherm case. The solution assumes that, initially, the system is at sorption equilibrium. The external boundary condition (i.e., at the particle surface) was alternated to

simulate the experimental protocol: while the purger was on, there was a constant zero concentration at the particle boundary; while the purger was off, the concentration in the volume surrounding the particles was allowed to increase until either the concentration gradient decreased to zero or the purger was switched on again. These conditions are

$$C_r(r = a) = 0 \quad (t_1)_i \leq t \leq (t_2)_i \quad (10)$$

$$C_r(r = a) = \frac{(M_x^p)_i - (M_x^p)_t}{V_e} \quad (t_2)_i < t < (t_1)_{i+1} \quad (11)$$

where $(M_x^p)_i$ is the intraparticle mass remaining after purge number i [–], $(M_x^p)_t$ is the intraparticle mass remaining after time t [–], $(t_1)_i$ is the starting time for purge number i [T], $(t_2)_i$ is the ending time for purge number i [T], V_e is the external volume surrounding the intraparticle zone [L³], and a is the particle radius [L]. For both conditions, the volume surrounding the particles is assumed to be well mixed. At the particle center, the condition of symmetry of the concentration profiles was maintained at all times:

$$\frac{\partial C_r(r = 0)}{\partial r} = 0 \quad (12)$$

A computer program (Fortran) was developed to execute the finite difference scheme. The numerical approximation was verified using the analytical solutions to the problems of diffusion from a sphere with a constant zero boundary condition and diffusion from a sphere into a well-mixed solution of limited volume (57). The spherical diffusion model was coupled with a fitting routine which determined the value of the effective pore diffusion coefficient (D_p) that minimized the mean squared error about the observed desorption data. Details about the code verification and fitting routine are available elsewhere (56).

Instantaneously Desorbing Fraction. For some of the samples, there was marked discrepancy between simulated and observed mass remaining immediately following the initial purging episode. Given the magnitude of the apparent diffusion coefficients observed in these particles, mass transfer from within the particles could not account for the discrepancy. One interpretation of such a phenomenon is that a portion of the sorbed compound is more readily accessible and desorbs very rapidly. The option for the release of an instantaneously desorbing fraction, X_i (–), was added to the batch model.

The X_i values were determined as the fractional difference between the first set of fitting simulations (for $X_i = 0$) and the observed first purge results. The X_i values were then employed in a second set of fitting runs. The nonzero X_i value forced the simulations to match observations at the time of the first purge and tended to reduce the D_p value necessary to achieve given mass removal over a given time (i.e., X_i became a second fitting parameter for these runs). However, it should be noted that the two-parameter fitting procedure used here is not completely consistent with that employed by Ball and Roberts (41).

Freundlich Isotherm Effects. A final set of D_p and χ_e values were determined for the Borden samples employing the version of the model allowing nonlinearity in the equilibrium relationship. The simulations incor-

porated the Freundlich isotherm parameters of Ball and Roberts (49), both for the entire range of concentrations ($1/n \approx 0.8$) and the low concentration range ($1/n \approx 0.9$). Although these parameters were reported for the Borden bulk only, the Freundlich exponent values, $1/n$, were used in the fitting runs involving the individual size fractions as well. The Freundlich sorption capacity coefficients (K_F) were converted from the linear coefficients (K_d) of the appropriate size fraction by equating the Freundlich isotherm expression with the linear isotherm expression at the equilibrium concentration (C_e), given the value of the exponent.

Error Propagation. In the intermittent purge results, each datum depends on the previous data and requires cumulative accounting. The data analysis included a standard treatment of error propagation, incorporating the experimental errors associated with the experimental sequence. Studies of the uncertainty associated with each mass addition or measurement indicated that the uncertainty associated with the initial sample spiking with ^{14}C -labeled PCE was the primary contributor to the overall uncertainty of the results (56). Of secondary importance was the uncertainty associated with the liquid scintillation counting of low-level yields from the later purges (approximately three times background levels).

Data Analysis

Raw data obtained from the intermittent purging procedure are in the form of radioactivity (DPM) and are related to the contaminant mass (PCE) by the specific activity (M_x/DPM). At the end of the purging sequence and scintillation extraction, the sum of the initial supernatant measurements and the purge and extraction recoveries were used to complete a ^{14}C mass balance for the individual samples. The measured value used to discriminate between valid and invalid samples was the discrepancy between the mass remaining following the final purge, and the ultimate release in the scintillation fluid extraction was defined as the measured fractional loss from each sample (F_L), i.e., the ratio of the DPM lost in a sample to the DPM added to the system (M_0). The F_L value accounts for the experimental losses accumulated during the spiking, cracking, purging, and extracting steps of the procedure.

The K_d value for each sample was estimated from its aqueous activity prior to the initial purge. The value was compared to the K_d value estimated from the sum of the postinitial purging yields and the scintillation extraction yields. Values determined by the two estimating procedures did not differ significantly. The K_d (or equivalent Freundlich parameters) values were used, in conjunction with the physical particle characteristics, to calculate the sample internal retardation factor (R_{int}) value and to determine the best-fitting D_p value for the individual contaminant release curves.

Typical results from the desorption rate studies are shown in Figure 2, which depicts the ^{14}C -labeled PCE remaining for a single sample. The raw data have been normalized by the total sample activity (M_0). Each datum on the plot represents the labeled compound recovered in each scintillation fluid trap. In general, the quantities yielded by the first purging episode represented a relatively large fraction of the total mass recovery. Presumably, the mass captured by the first purge is the mass stripped from

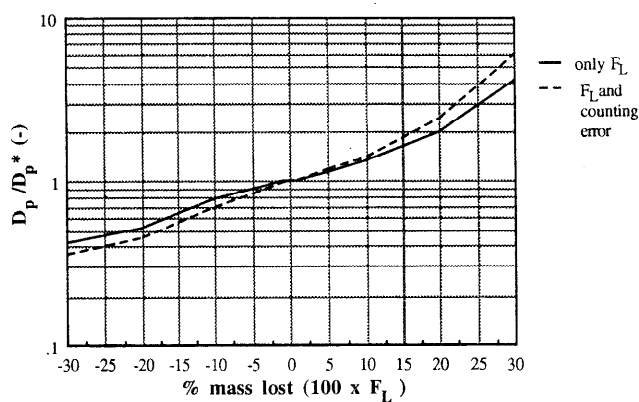


Figure 3. Effect of experimental mass loss (F_L) on D_p estimate for radial diffusion model and Borden -20+40 preliminary sample (D_p^* = the best fitting D_p value for the case of no mass loss).

the aqueous interparticle phase, but may include an instantaneously desorbing fraction. The next several purges also yielded relatively large fractions of the total mass.

The second set of data in Figure 2, indicating an increase in the fractional mass released with time, corresponds to the final recovery of ^{14}C -labeled PCE by the scintillation fluid extraction method (56). These data represent the repetitive counting of duplicate subsamples of the solids removed following the final purging episode. The extraction data appeared to demonstrate a rate behavior that is similar to that manifested in the purging results (67).

Using the batch pore diffusion model, a sensitivity analysis was undertaken to quantify the effects of F_L alone and combined with the cumulative scintillation counting errors on the desorption rate interpretation. Raw data from a preliminary experiment (Borden -20+40 with PCE) resulted in a F_L value of 0.02, a value approximately within the experimental uncertainty of the mass added to the system (M_0). The data from this experiment were used to determine the sensitivity of the best-fitting pore diffusion coefficient (D_p) value to the F_L value. The results of the sensitivity analysis are shown in Figure 3, which shows the ratio of the best-fitting D_p value obtained for a given F_L value to the D_p value obtained for the ideal case (perfect balance between mass added and mass recovered, or $F_L = 0$). Deviation from unity reflects the degree to which the best-fitting D_p value deviates from the value expected given no experimental uncertainty. As the plots indicate, there is a noticeable deviation for even the smallest F_L value. In other words, as the experimental mass balance deviates from unity, the certainty of the model fit's uniqueness decreases. Incorporation of the scintillation counting error in the fitting exercises (dashed line in Figure 3) contributed a slight degree of additional uncertainty.

An observed F_L value of 10% limits the relative uncertainty of the diffusion rate estimates to approximately 30% (i.e., ± 0.30 [expected D_p value]) and was chosen arbitrarily as acceptable for the model interpretation of the intermittent purging data. The F_L values for the majority of the samples in the study (and all samples included in this paper) were significantly less than 10%.

Results

The experimental results are presented in terms of the measured equilibrium and rate parameters. The observed equilibrium distribution coefficient (K_d) values are com-

Table 2. Comparison of Observed Sorbent-PCE Equilibrium Characteristics with Previous Results

sample ID	$t_{0.95}$ (day) ^a	equilibrium time (day)	equilibrium concn C_e ($\mu\text{g/L}$) ^b	sorption K_d (mL/g) ^c	sorption retardation $R_{int}(-)$ ^d	single-point K_d (mL/g)	single-point retardation $R_{int}(-)$ ^d
-12+20(A)	55	110	26 ± 3	8.0 ± 1.1	430	4.01 ± 0.37	220
-12+20(B)		220	29 ± 3			3.46 ± 0.33	190
-12+20(C)		200	21 ± 3			4.77 ± 0.46	260
-20+40(A)	20	90	51 ± 4	2.9 ± 0.29	430	1.24 ± 0.13	175
-20+40(B)		110	30 ± 3			1.33 ± 0.14	190
-40+60(A)	9.3	200	58 ± 5	1.2 ± 0.14	190	0.35 ± 0.065	50
-40+60(B)		210	81 ± 6			0.51 ± 0.076	75
-60+80(A)	8.8	140	53 ± 4	0.55 ± 0.054	130	0.44 ± 0.073	100
-60+80(B)		200	65 ± 5			0.73 ± 0.083	180
-80+120(A)	2.8	100	75 ± 6	0.30 ± 0.008	60	0.59 ± 0.077	120
-80+120(B)		60	59 ± 5			0.34 ± 0.070	70
-120+200(A)	1.6	220	52 ± 4	0.26 ± 0.023	47	0.46 ± 0.078	80
-200(A)	1.7	140	42 ± 4	0.82 ± 0.056	630	0.67 ± 0.098	520
-200(B)		200	40 ± 4			0.74 ± 0.098	570
-200(C)		200	67 ± 10			0.73 ± 0.18	570
bulk:							
2bulk1	7.0	200	48 ± 4	0.74 ± 0.14	160	0.55 ± 0.080	115
2bulk3		200	48 ± 4			0.56 ± 0.080	115
pulvd bulk							
6PB5	ND ^e	200	73 ± 8	ND	ND	0.65 ± 0.19	135
6PB6		200	74 ± 9			0.62 ± 0.20	130

^a Time reported (41) for apparent K_d to reach 95% of K_d (equilibrium value). ^b Concentration determined by measurement of the sample supernatant prior to initial purge (± 1 SD). ^c Combined pulverized and unaltered results; final aqueous concentrations below 30 $\mu\text{g/L}$ (49). ^d This work. ^e Not determined; $t_{0.95}$ determined for the pulverized -20+40 fraction was 0.33 day.

pared to equilibrium isotherm results from the previous study (49). These single-point K_d values, along with the physical particle characteristics (Table 1), provide the means by which to independently estimate the internal retardation factor (R_{int}) for each sample. Given these estimates, the analysis focuses on a pore diffusion interpretation of the desorption rate data. Values of the best-fitting pore diffusion coefficients are compared with the corresponding values generated in the previous study of sorptive uptake (41).

Single-Point Distribution Coefficients. Table 2 provides a summary of the single-point K_d values derived from the purging samples. As was discussed previously, the equilibration times were chosen to be at least twice the reported $t_{0.95}$ value of Ball and Roberts (41), although most of the samples were equilibrated for much greater periods of time. The final concentrations shown for the Borden bulk samples were approximately within the range reported by Ball and Roberts (49) for lower concentrations (30–50 $\mu\text{g/L}$). Over this relatively narrow concentration range, Ball and Roberts reported relatively slight isotherm nonlinearities ($1/n \approx 0.90$).

There were several notable discrepancies between the single-point distribution coefficients or K_d values generated in this study and the multiple-point (isotherm) values reported by Ball and Roberts (49). The largest differences were found with the largest three size fractions (-12+20, -20+40, and -40+60 mesh), for which the single-point K_d values were only about one-third to one-half of the isotherm-based values. The discrepancies were smaller among the other fractions, with the possible exception of the -120+200 fraction, which in a single measurement exhibited a single-point K_d value almost two times greater than the value reported by Ball and Roberts (49). The general trend seen in the comparison of the single-point K_d values and those derived from previous sorption studies are also seen in the calculated internal retardation factor values (R_{int}) shown in Table 2.

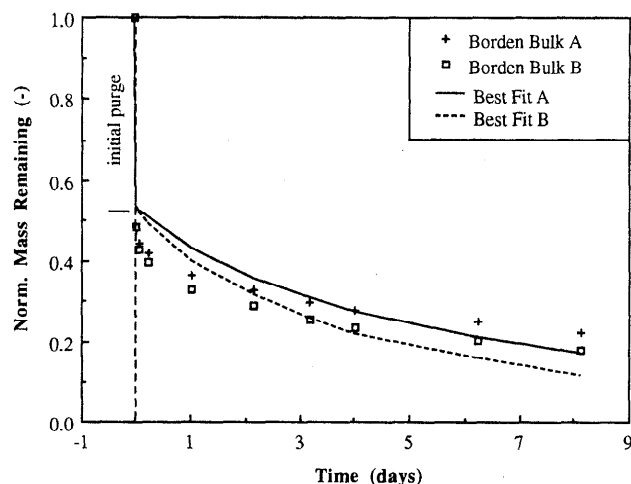


Figure 4. Duplicate Borden bulk intermittent purge samples and pore diffusion model simulation (Note: The difference between the simulated and observed initial purge of the aqueous phase was interpreted as an instantaneously desorbing fraction).

Desorption Rates. Figure 4 contains plots of duplicate Borden bulk samples, including the first datum (representing conditions prior to the first purge) and the best-fitting model simulations. Qualitatively, the model described the dynamics of the system reasonably well, capturing the relatively fast initial release from the sample and the relatively slow release that followed. However, it is apparent that the model underestimates the desorption rate at early times and overestimates the rate at later times. This aspect of the simulations may be due, in part, to the wide range of particle sizes associated with the bulk sample (68–70). Model fits were found to be unique, based on minimizing the mean-squared residuals (56).

Figure 5 shows plots and best-fitting simulations for several of the Borden size fractions. In these plots, the datum and simulation at the time of the initial purge are omitted in order to focus attention on the desorption behavior. The simulations incorporated linear isotherms

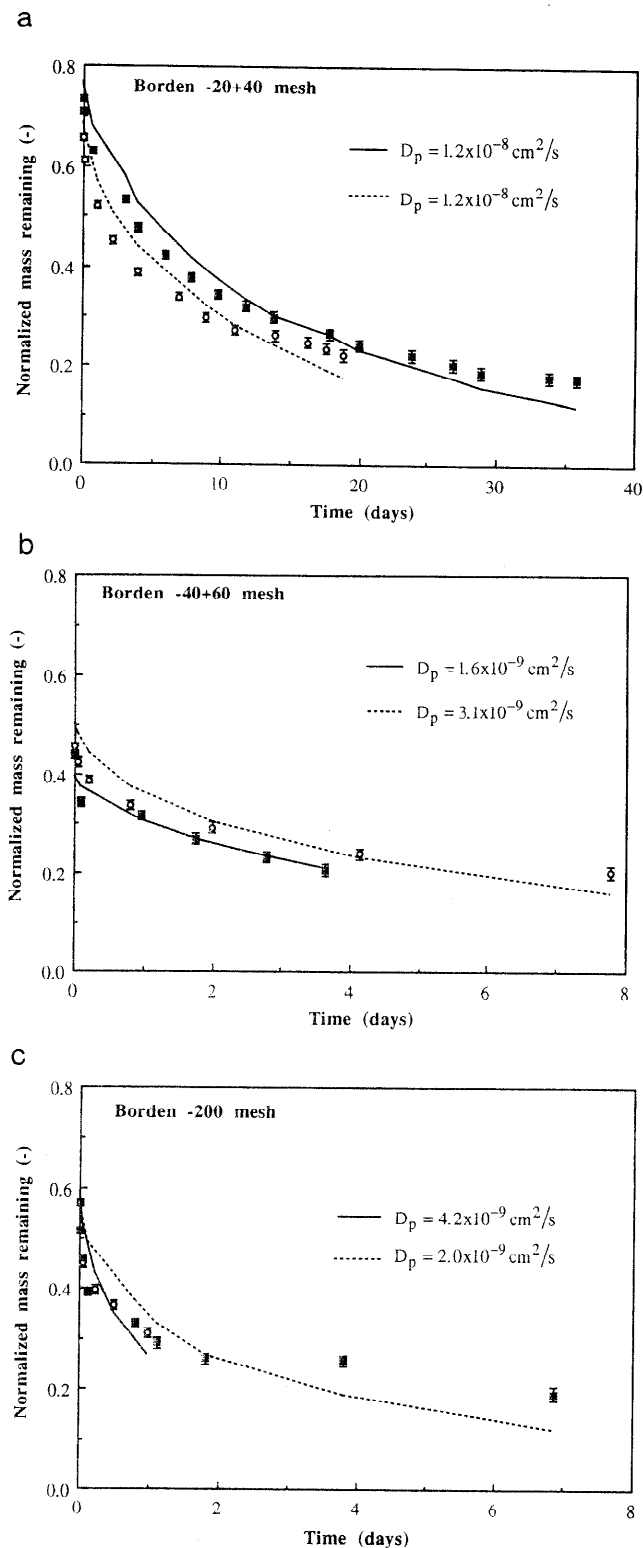


Figure 5. Duplicate Borden -20+40 (a), -40+60 (b), and -200 (c) mesh samples: intermittent purge results and pore diffusion model simulations (linear isotherm and no instantaneously desorbing fraction).

and no instantaneously desorbing fraction. The initial underestimation and final overestimation observed in the bulk simulations (Figure 4) are also evident among the size fraction simulations but, with the exception of the -200 fraction, to a lesser extent.

Including the second fitting parameter (X_i) improved the model fits at early times and lowered the best fitting D_p values slightly, in accord with Ball and Roberts (41). A comparison of model performances (with and without

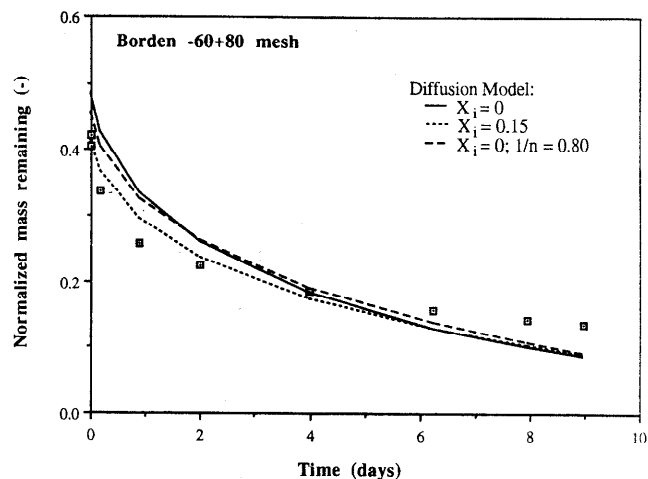


Figure 6. Borden -60+80 mesh intermittent purge results and pore diffusion model simulation (linear isotherm, linear isotherm with instantaneously desorbing fraction, and nonlinear isotherm).

the instantaneous fraction) is depicted in Figure 6. Simulations adjusted to include the nonlinear isotherm improved the model's fit of the data only marginally; typical results are also shown in Figure 6 (for the case of $1/n = 0.80$). The resulting best-fitting D_p values for the nonlinear isotherm simulations were approximately 10% larger than those determined for the linear isotherm simulations.

A summary of the results from the simulations for linear isotherms is provided in Table 3. Included with the results from this study are the corresponding uptake parameters reported by Ball and Roberts (41). In most cases, the values of D_p determined from the desorption data were about one-fourth to one-half of those determined from the sorption data. Accordingly, the values calculated for the effective tortuosity factor, χ_e , were greater for the desorption study. Of the 17 desorption samples shown in Table 3, only two samples, one -12+20 mesh and one -200 mesh, displayed desorption-based D_p values that were greater than the sorption-based values.

Discussion

Single-Point K_d Values. For the single-point K_d values, several of the size fractions demonstrated a substantially lower sorption capacity than was expected based on the previous equilibrium study of Ball and Roberts (49). One explanation for this is that the original cores for the two sets of samples were different. Mackay *et al.* (62) reported K_d values for a set of 12 homogenized core samples that differed by as much as a factor of 2. However, most of the 12 core samples yielded K_d values that were within about 30% of the values for the other cores.

A more likely explanation of the discrepancies between the K_d values from the different studies is related to the concentration ranges observed in the respective studies and the isotherm nonlinearity. Single-point K_d estimates are dependent on the equilibrium concentration, if the isotherm is nonlinear. In a column study with a single Borden sand fraction (-40+60 mesh), Young and Ball (20) employed K_d values as approximations of the nonlinear isotherm ($1/n = 0.79$) over two concentration ranges: a K_d value of 0.35 mL/g gave the best linear approximation of the data between final aqueous concentrations of 36-795

Table 3. Comparison of Desorption-Based Pore Diffusion Coefficient Estimates with Sorption-Based Values

sample ID	desorption X_i	desorption D_p (cm ² /s) ^a	desorption χ_e ^b	sorption X_i	sorption D_p (cm ² /s) ^c	sorption χ_e	$(D_p)_d/(D_p)_s$
-12+20(A)	0	2.0×10^{-8}	380	0	4.8×10^{-8}	160	0.42
-12+20(B)	0	5.2×10^{-8}	140				1.08
-12+20(B)	0.03	3.6×10^{-8}	200				0.75
-12+20(C)	0	5.2×10^{-8}	140				1.08
-20+40(A)	0	1.2×10^{-8}	630	0	3.6×10^{-8}	210	0.33
	0.04	1.1×10^{-8}	690	0.01	3.4×10^{-8}	220	0.32
-20+40(B)	0	1.2×10^{-8}	630				0.33
	0.05	1.1×10^{-8}	690				0.32
-40+60(A)	0	1.6×10^{-8}	4700	0	1.1×10^{-8}	680	0.15
-40+60(B)	0	3.1×10^{-9}	2400	0.04	7.9×10^{-9}	950	0.28
	0.10	2.2×10^{-9}	3400				0.28
-60+80(A)	0	1.5×10^{-9}	5000	0	4.2×10^{-9}	1800	0.36
	0.05	1.2×10^{-9}	6300	0.06	3.3×10^{-9}	2300	0.50
-60+80(B)	0	2.1×10^{-9}	3600				
	0.15	1.8×10^{-9}	4200				
-80+120(A)	0	7.4×10^{-10}	10000	0	3.2×10^{-9}	2300	0.23
	0.11	5.5×10^{-10}	8800	0.18	1.6×10^{-9}	4700	0.27
-80+120(B)	0	8.5×10^{-10}					
	0.12	5.6×10^{-10}					
-120+200(A)	0	7.2×10^{-10}	10400	0	1.8×10^{-9}	4200	0.40
	0.11	4.6×10^{-10}		0.22	7.5×10^{-10}	10000	
-200(A)	0	2.0×10^{-9}	3800	0	8.0×10^{-9}	1000	0.25
	0.02	1.6×10^{-9}	4800	0.31	2.6×10^{-9}	3100	0.62
-200(B)	0	4.2×10^{-9}	1800				0.53
	0.05	2.1×10^{-9}	3600				0.81
-200(C)	0	7.7×10^{-9}	1000				0.96
	0.19	4.1×10^{-9}	1900				1.58
bulk	0	2.7×10^{-9}	2800	0	5.3×10^{-9}	1400	0.51
	0	3.9×10^{-9}	1900	0.10	3.5×10^{-9}	2100	0.74

^a Shown are the best fits, for all samples, obtained with the intermittent purge model (assuming internal retardation factors from Table 2 and no instantaneously desorbing fraction). ^b Effective tortuosity factor $\chi_e = D_b/D_p$ where D_b is the bulk aqueous diffusivity of PCE: 7.5×10^{-6} cm²/s. ^c The upper limit value from Ball and Roberts (14) model 1 (assuming no instantaneous fraction and internal retardation factors from measured K_d and porosity).

$\mu\text{g/L}$; 1.2 mL/g gave the best linear approximation over a much lower range (2.9–4.3 $\mu\text{g/L}$; ref 49). The K_d values of the -40+60 size fraction used in this study (0.35 and 0.51 mL/g, from Table 2) were observed at final concentrations of 58 and 81 $\mu\text{g/L}$, respectively, and are consistent with values observed by Young and Ball (for graphical comparison, see Figure 4a in ref 20).

Intermittent Purging Results. Perhaps the most significant results of this study concern the fact that the desorption-based D_p estimates were generally about 2–4 times less than the corresponding sorption based values (Table 3). If not accounted for in the rate determination procedure, nonlinear sorption could cause the measured value of the overall rate of desorption, characterized by the apparent diffusion coefficient (D_a), to be less than that of the rate of sorption (see Theory section). However, the D_p estimates should be independent of the equilibrium isotherm and the same for both the sorption- and desorption-based estimates if the isotherm nonlinearity is incorporated into the rate-fitting model. In this study, there was not a significant difference between D_p values based on the nonlinear equilibrium version of the batch model and those based on the linear equilibrium version.

If the differences between the measured sorption and desorption rates are real, i.e., not experimental artifacts, then the basis for the diffusion model must be scrutinized more carefully. Possible explanations are (1) a significant fraction of the sand grains' microporosity offers a more severely restricted and possibly sterically hindered diffusion path and (2) a true hysteretic phenomenon affects the sorption and desorption rates, as suggested by Farrell and Reinhard (77).

Diffusional Interpretations. The effective diffusivities for the Borden sand fractions implied effective

tortuosity values that were more than 1 order of magnitude greater than would be predicted using the simple inverse relation with intraparticle porosity (eq 8). This result is not surprising for there is abundant evidence that very slow diffusion occurs in highly constricted pore networks. Effective diffusivities on the order of 10^{-12} – 10^{-11} cm²/s have been reported in the zeolite literature (e.g., refs 54 and 71). Nitrogen adsorption studies with the Borden sand indicated the presence of micropores of molecular dimensions. It is reasonable to assume that effective diffusivities in these pores would be on the order of 10^{-12} cm²/s and would act to weigh the measured effective diffusivity value toward a lower value. If this is true, then the effective diffusivity values measured in this study are average values related to the intraparticle pore size distributions. This mechanism is reasonable in view of the measured D_p values underestimating release at early times (presumably, when the measured D_p value is less than the local value for the initially accessed pores) and overestimating at later times (when the measured D_p value is greater than the local value for the finally accessed pores).

Current methods for measuring the spatial distribution of intraparticle pores are inadequate. Combining nitrogen desorption and mercury intrusion data yields only an intraparticle pore volume and a rough estimate of the range of pore sizes and their contribution to the total pore volume. There is not a unique spatial distribution to be inferred from the observed behavior. Fractal-type geometries may provide an appropriate mathematical description of such pore networks: relatively large, accessible pores branching to smaller, more constricted pores; or fractures, with apertures, relatively wide in the center, extending and constricting laterally. Although scanning electron microscopy (SEM) provides qualitative evidence of particular

geometries, conclusive evidence must await further method development.

It is important to emphasize that the limitations of the method in this study (i.e., measuring the rate of mass flux out of the particles) precludes conclusive verification of the pore diffusion mechanism. Others have offered alternative mechanisms to explain nonequilibrium sorption behavior. Ball and Roberts (41, model 2) propose a second pore diffusion model interpretation by attributing the internal retardation phenomenon solely to a fraction of the grains that are sorbing. With the Borden sand, they hypothesized that the sorbing grains were the ones containing a significant fraction of calcareous rock fragments (for Borden sand mineralogy, see ref 60) and employed a single R_{int} value of 430 for PCE.

Another mechanistic interpretation represents a departure from the pore and surface diffusion interpretations, associating slow sorption/desorption behavior with the diffusion of solute through soil organic matter (25, 72-74). However, this mechanism appears unlikely to occur in aquifer solids characterized by extremely low organic carbon fractions (41, 75).

Potential Applicability to Site Characterization.

One of the underlying motivations for this work was to advance the capabilities for predictive modeling of solute transport at contaminated sites. To this end, the intermittent purge and scintillation extraction methods can provide reasonably accurate results for a large number of samples. This capacity could be advantageous in the characterization of a large, heterogeneous aquifer.

The equilibration times required in this study, for compounds that are relatively weakly sorbing, were somewhat long from the standpoint of an actual field characterization. For all but the largest size fractions, the much shorter equilibration times would have sufficed. However, more strongly sorbing compounds would probably render the duration of the parametrization techniques unreasonably long. With a better understanding of the underlying mechanisms, it may be possible to work with pulverized samples (41, 49) in conjunction with short-term rate studies using unaltered samples to obtain the desired desorption rate parameters (53).

Conclusions

Development of a batch procedure for measuring desorption rates focused on achieving two objectives: (1) to test the hypothesis that the sorption and desorption rates are the same in a sandy aquifer material and (2) to do so with a method that is suitable for large numbers of samples. The intermittent purging method was developed for measuring the effective pore diffusion coefficient (D_p) in aquifer particles. The intermittent purging apparatus employed flame-sealed glass ampules, allowing for the long-term equilibration of a solute-sorbent system. The method also provided an estimate for the equilibrium distribution coefficient (K_d) for each sample. A second procedure, scintillation fluid extraction, provided completion of the mass recovery from the intermittent purging samples. The main conclusions emanating from this work are as follows:

(1) The intermittent purging technique (followed by scintillation fluid extraction) appears to be a feasible method for measuring desorption rate parameters.

(2) Desorption rate parameters measured for Borden sand and PCE were 2-4 times less than those determined

in the previous uptake experiments. This conclusion is far from definitive: a combination of experimental uncertainty, materials, and method alterations may account for the observed differences.

Acknowledgments

This project was funded through a grant from the Western Region Hazardous Substance Research Center of the United States Environmental Protection Agency. The article has not been subjected to EPA review and, therefore, does not necessarily reflect their views. Additional support from the American Geophysical Union (Horton Research Grant) and the California Association of Civil Engineers is also gratefully acknowledged.

Literature Cited

- (1) Bahr, J. M. *J. Contam. Hydrol.* 1989, 4, 205.
- (2) Mackay, D. M.; Cherry, J. A. *Environ. Sci. Technol.* 1989, 23, 630.
- (3) Harmon, T. C.; Semprini, L.; Roberts, P. V. *J. Environ. Eng.* 1992, 118, 666.
- (4) Pignatello, J. J. *J. Environ. Qual.* 1987, 16, 307.
- (5) Rijnaarts, H. H. M.; Bachmann, A.; Jumelet, J. C.; Zehnder, A. J. B. *Environ. Sci. Technol.* 1990, 24, 1349.
- (6) Semprini, L.; Hopkins, G. D.; Roberts, P. V.; Grbić-Galić, D.; McCarty, P. L. *Ground Water* 1991, 29, 239.
- (7) van Genuchten, M. Th.; Wierenga, P. J. *Soil Sci. Soc. Am. Proc.* 1974, 38, 29.
- (8) van Genuchten, M. Th.; Wierenga, P. J. *Soil Sci. Soc. Am. J.* 1976, 40, 473.
- (9) Nkedi-Kizza, P.; Biggar, J. W.; Selim, H. M.; van Genuchten, M. Th.; Wierenga, P. J.; Davidson, J. M.; Neilson, D. R. *Water Resour. Res.* 1984, 20, 1123.
- (10) Crittenden, J. C.; Hutzler, N. J.; Geyer, D. G.; Oravitz, J. L.; Friedman, G. *Water Resour. Res.* 1986, 22, 2714.
- (11) van Genuchten, M. Th.; Wierenga, P. J.; O'Connor, G. A. *Soil Sci. Soc. Am. J.* 1977, 41, 278.
- (12) Rao, P. S. C.; Davidson, J. M.; Jessup, R. E.; Selim, H. M. *Soil Sci. Soc. Am. J.* 1979, 43, 22.
- (13) Nkedi-Kizza, P.; Biggar, J. W.; van Genuchten, M. Th.; Wierenga, P. J.; Selim, H. M.; Davidson, J. M.; Nielson, D. R. *Water Resour. Res.* 1983, 19, 691.
- (14) Nkedi-Kizza, P.; Brusseau, M. L.; Rao, S. C.; Hornsby, A. G. *Environ. Sci. Technol.* 1989, 23, 814.
- (15) Miller, C. T.; Weber, W. J., Jr. *J. Contam. Hydrol.* 1986, 1, 243.
- (16) Hutzler, N. J.; Crittenden, J. C.; Gierke, J. S.; Johnson, A. S. *Water Resour. Res.* 1986, 22, 285.
- (17) Roberts, P. V.; Goltz, M. N.; Summers, S. R.; Crittenden, J. C.; Nkedi-Kizza, P. *J. Contam. Hydrol.* 1987, 1, 375.
- (18) Lee, L. S.; Rao, P. S. C.; Brusseau, M. L.; Ogwada, R. A. *Environ. Toxicol. Chem.* 1988, 7, 779.
- (19) Miller, C. T.; Weber, W. J., Jr. *Water Res.* 1988, 22, 465.
- (20) Young, D. F.; Ball, W. P. *Environ. Prog.* 1994, 13, 9.
- (21) Weber, W. J., Jr.; Miller, C. T. *Water Res.* 1988, 22, 457.
- (22) Karickhoff, S. W. *Contaminants and Sediments*; Baker, R. A., Ed.; Ann Arbor Science: Ann Arbor, MI, 1980; Vol. 2, Chapter 11.
- (23) Karickhoff, S. W.; Morris, K. R. *Environ. Toxicol. Chem.* 1985, 4, 466.
- (24) Rao, P. S. C.; Davidson, J. M. In *Environmental Impact of Nonpoint Source Pollution*; Overcash, M. R., Davidson, J. M., Eds.; Ann Arbor Science: Ann Arbor, MI, 1980; pp 23-67.
- (25) Pignatello, J. J. In *Reactions and Movement of Organic Chemicals in Soils*; Sawhney, B. L., Brown, K., Eds.; Soil Science Society of America, Inc.: Madison, WI, 1989; Chapter 3.
- (26) Karickhoff, S. W.; Brown, D. S. *J. Environ. Qual.* 1978, 7, 246.
- (27) Gschwend, P. M.; Wu, S.-C. *Environ. Sci. Technol.* 1985, 19, 90.

- (28) Harmon, T. C.; Ball, W. P.; Roberts, P. V. In *Reactions and Movement of Organic Chemicals in Soils*; Sawhney, B. L., Brown, K., Eds.; Soil Science Society of America, Inc.: Madison, WI, 1989; Chapter 16.
- (29) Ball, W. P.; Roberts, P. V. In *Organic Substances in Sediments and Water*; Baker, R. A., Ed.; Lewis Publishers, Inc.: Chelsea, MI, 1991; Vol. 2, Chapter 13.
- (30) Miller, C. T.; Pedit, J. A. *Environ. Sci. Technol.* **1992**, *26*, 1417.
- (31) Steinberg, S. M.; Pignatello, J. J.; Sawhney, B. L. *Environ. Sci. Technol.* **1987**, *21*, 1201.
- (32) Sawhney, B. L.; Pignatello, J. J.; Steinberg, S. M. *J. Environ. Qual.* **1988**, *17*, 149.
- (33) Pavlostathis, S. G.; Mathavan, G. N. *Environ. Sci. Technol.* **1992**, *26*, 532.
- (34) Chrysikopoulos, C. V.; Kitanidis, P. K.; Roberts, P. V. *Water Resour. Res.* **1990**, *26*, 437.
- (35) Chrysikopoulos, C. V.; Kitanidis, P. K.; Roberts, P. V. *Transp. Porous Media* **1992**, *7*, 163.
- (36) Chrysikopoulos, C. V.; Kitanidis, P. K.; Roberts, P. V. *Water Resour. Res.* **1992**, *28*, 1517.
- (37) Valocchi, A. J. *Water Resour. Res.* **1989**, *25*, 273.
- (38) Oliver, B. G. *Chemosphere* **1985**, *14*, 1087.
- (39) Wu, S.-C.; Gschwend, P. M. *Environ. Sci. Technol.* **1986**, *20*, 717.
- (40) Brusseau, M. L.; Jessup, R. E.; Rao, P. S. C. *Environ. Sci. Technol.* **1990**, *24*, 727.
- (41) Ball, W. P.; Roberts, P. V. *Environ. Sci. Technol.* **1991**, *25*, 1237.
- (42) Johnson, J. A.; Farmer, W. J. *Soil Sci.* **1993**, *155*, 92.
- (43) Grathwohl, P.; Reinhard, M. *Environ. Sci. Technol.* **1993**, *27*, 2360.
- (44) Farrell, J.; Reinhard, M. *Environ. Sci. Technol.* **1994**, *28*, 63.
- (45) Karickhoff, S. W.; Brown, D. S.; Scott, T. A. *Water Res.* **1979**, *13*, 241.
- (46) Schwarzenbach, R. P.; Westall, J. *Environ. Sci. Technol.* **1981**, *15*, 1360.
- (47) Chiou, C. T.; Porter, P. E.; Schmedding, D. W. *Environ. Sci. Technol.* **1983**, *17*, 227.
- (48) Curtis, G. P.; Reinhard, M.; Roberts, P. V. *Geochemical Processes at Mineral Surfaces*; Davis, J. A., Hayes, K. F., Eds.; American Chemical Society: Washington, DC, 1986; p 191.
- (49) Ball, W. P.; Roberts, P. V. *Environ. Sci. Technol.* **1991**, *25*, 1223.
- (50) Atkins, P. W. *Physical Chemistry*, 3rd ed.; W. H. Freeman and Co.: New York, 1986; pp 777-782.
- (51) Wilke, C. R.; Chang, P. *AIChE J.* **1955**, *1*, 264.
- (52) Wakao, N.; Smith, J. M. *Chem. Eng. Sci.* **1962**, *17*, 825.
- (53) Harmon, T. C.; Roberts, P. V. *Environ. Prog.* **1994**, *13*, 1.
- (54) Satterfield, C. N.; Colton, C. K.; Pitcher, W. H., Jr. *AIChE J.* **1973**, *19*, 628.
- (55) Chantong, A.; Massoth, F. E. *AIChE J.* **1983**, *29*, 725.
- (56) Harmon, T. C. Ph.D. Dissertation, Stanford University, 1992.
- (57) Crank, J. *The Mathematics of Diffusion*, 2nd ed.; Oxford University Press: New York, 1975; Chapter 6.
- (58) Roberts, P. V.; Goltz, M. N.; Mackay, D. M. *Water Resour. Res.* **1986**, *22*, 2047.
- (59) Mackay, D. M.; Freyberg, D. L.; Roberts, P. V.; Cherry, J. A. *Water Resour. Res.* **1986**, *22*, 2017.
- (60) Ball, W. P.; Buehler, C.; Harmon, T. C.; Mackay, D. M.; Roberts, P. V. *J. Contam. Hydrol.* **1990**, *5*, 1.
- (61) Curtis, G. P.; Roberts, P. V.; Reinhard, M. *Water Resour. Res.* **1986**, *22*, 2059.
- (62) Mackay, D. M.; Ball, W. P.; Durant, M. G. *J. Contam. Hydrol.* **1986**, *1*, 119.
- (63) Criddle, C. S.; McCarty, P. L.; Elliott, M. C.; Barker, J. F. *J. Contam. Hydrol.* **1986**, *1*, 133.
- (64) Bouwer, E. J.; Rittmann, B. E.; McCarty, P. L. *Environ. Sci. Technol.* **1981**, *15*, 596.
- (65) Bouwer, E. J.; McCarty, P. L. *Appl. Environ. Microbiol.* **1983**, *45*, 1286.
- (66) Nicholson, R. V.; Cherry, J. A.; Reardon, E. J. *J. Hydrol.* **1983**, *63*, 131.
- (67) Harmon, T. C.; Roberts, P. V. In *Proceedings of the Water Environment Federation 66th Annual Conference*; Anaheim, CA, Oct. 3-7, 1993; Water Environment Federation: Alexandria, VA, 1993; Vol. 5, p 97.
- (68) Wu, S.-C.; Gschwend, P. M. *Water Resour. Res.* **1988**, *24*, 1373.
- (69) Fong, F. K.; Mulkey, L. A. *Water Resour. Res.* **1990**, *26*, 843.
- (70) Fong, F. K.; Mulkey, L. A. *Water Resour. Res.* **1990**, *26*, 1291.
- (71) Roberts, P. V.; York, R. *Ind. Eng. Chem. Process Des. Dev.* **1967**, *6*, 516.
- (72) Brusseau, M. L.; Rao, P. S. C. *Chemosphere* **1989**, *18*, 1691.
- (73) Brusseau, M. L.; Rao, P. S. C., *Crit. Rev. Environ. Control* **1989**, *19*, 33.
- (74) Brusseau, M. L.; Reid, M. E. *Chemosphere* **1991**, *22*, 341.
- (75) Brusseau, M. L.; Larsen, T.; Christensen, T. H. *Water Resour. Res.* **1991**, *27*, 1137.
- (76) Mathews, A. P.; Zayas, I. *J. Environ. Eng.* **1989**, *115*, 41.
- (77) Farrell, J.; Reinhard, M. *Environ. Sci. Technol.* **1994**, *28*, 53.

Received for review October 19, 1993. Revised manuscript received May 19, 1994. Accepted May 26, 1994.*

* Abstract published in *Advance ACS Abstracts*, July 1, 1994.